Journal of Porphyrins and Phthalocyanines
J. Porphyrins Phthalocyanines 2020; **24**: 211–219
DOI: 10.1142/S1088424619500895

Published at https://www.worldscinet.com/jpp/

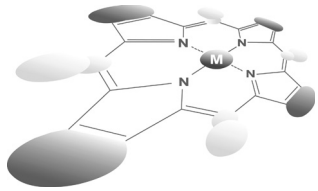

Singlet oxygen generation of subphthalocyanine-fused dimer and trimer

Rei Fujishiro[a], Hayato Sonoyama[a], Yuki Ide[a], Takuya Fujimura[a], Ryo Sasai[a], Nichole E. M. Kaufman[b], Zehua Zhou[b], M. Graça H. Vicente[b] and Takahisa Ikeue[a,*◊]

[a] *Department of Chemistry, Graduate School of Science and Engineering, Shimane University, 1060 Nishikawatsu, Matsue 690-8504, Japan*
[b] *Department of Chemistry, Louisiana State University, Baton Rouge, Louisiana 70803-1804, USA*

Dedicated to Professor Atsuhiro Osuka on the occassion of his 65th birthday.

Received 17 May 2019
Accepted 19 June 2019

ABSTRACT: Subphthalocyanine (SubPc) macrocycles are known as an interesting class of nonplanar aromatic dyes. Despite documented high fluorescence and singlet oxygen quantum yields, the properties of SubPcs in photodynamic therapy (PDT) are underestimated, because their absorption bands do not reach a significant wavelength range. With this in mind, we combined a SubPc ring and a SubPc ring by introducing a common benzene ring and obtained a SubPc dimer (**2**) and trimer (**3**) with the Q-band at the near-IR region, owing to the expansion of the π electron conjugated system. In this study, we reported $^1O_2$ generation abilities of **2** and **3** based on the applied absolute singlet oxygen quantum yields ($\Phi_{\Delta absolute}$). Subsequent research revealed that **2** and **3** showed the potential to generate $^1O_2$ to not only in toluene but also in DMSO. Although the photocytotoxicity of **2** and **3** were investigated upon photoirradiation with a low light dose of approximately 1.5 J/cm^2, **2** and **3** showed almost negligible toxic properties toward HEp2 cells.

KEYWORDS: subphthalocyanine dimer and timer, singlet oxygen generation, photocytotoxity, photodynamic therapy.

INTRODUCTION

Subphthalocyanines (SubPcs) are macrocyclic compounds composed of three diiminoisoindole units and central boron atoms. While many phthalocyanine metal complexes having several metal ions at their central vacancy have been known, only SubPcs boron complexes have been reported since the serendipitous discovery of Meller and Ossko in 1972 [1]. SubPcs have non-planar cone-shaped structures which are greatly distorted and differ from phthalocyanines (Pcs) with a high planar structure. SubPcs have 14π electron conjugated system and have received much attention owing to their characteristic non-planar structure and unique spectral and electronic properties. Recently, SubPcs have developed as functional materials in a variety of fields such as organic photovoltaics, organic LEDs, chemical sensors, organic thin film transistors, and non-linear optical materials [2].

The absorption bands of SubPcs feature a Q-band and a Soret-band similar to those of Pcs. The absorption bands of SubPcs shift to shorter wavelengths because of π-conjugated system, which is smaller than that of Pcs. The wavelength of the Q- and the Soret-band are at around 560 nm and 300 nm, respectively. The typical molar extinction coefficients (ε) of the Q- and the Soret-band are also in the case of SubPcs compared to Pcs and the typical ε values of the Q-band of SubPcs are approximately 10^4 $M^{-1}cm^{-1}$, whereas those of Pcs are approximately 10^5 $M^{-1}cm^{-1}$ [3, 4].

One of the most valuable applications of Pcs derivatives is as photosensitizer in photodynamic therapy (PDT) for cancer and other diseases. PDT related research has been actively pursued by many researchers

◊ SPP full member in good standing.

*Correspondence to: Takahisa Ikeue, email: ikeue@riko.shimane-u.ac.jp, tel.: +81 852-32-6423, fax: +81 852-32-6429.

since PDT treatments are minimally invasive procedures [5–7]. It is well known that Pcs derivatives are suitable for photosensitizers used in PDT owing to the Q-band absorption in the near-IR region (670–750 nm) which can penetrate deeply into tissues. [8, 9]. In the photoreaction mechanisms of PDT, the photo irradiations produce triplet state photosensitizers *via* intersystem crossing (ISC). The triplet state photosensitizer reacts with oxygen to generate reactive oxygen species (ROS), such as singlet oxygen ($^1O_2$) and free radicals. Significant damage to the cancer cells is obtained at great depth by ROS [5, 10, 11].

In the application of water-soluble Pc derivatives as photosensitizers in PDT, the aggregation behavior of Pcs arises as a result of highly planar structure and limits their efficiency as photosensitizers in PDT [12–14]. SubPcs have a nonplanar cone-shaped structure, high molar extinction coefficients (ε) of the Q-band, and a long triplet state lifetime. Therefore, these properties of the SubPcs could improve the efficiency of photosensitizers derived from the SubPcs compared to those derived from Pcs. However, a photosensitizer derived from SubPcs has a wavelength that does not reach the near-IR region. In 2002, Torres *et al*. and Kobayashi *et al*. combined a SubPc ring and a SubPc ring by introducing a common benzene ring and obtained a SubPc dimer and trimer with the Q-band at the near-IR region, owing to the expansion of the π electron conjugated system [15, 16].

Herein, we synthesized a SubPc dimer (**2**) and trimer (**3**), which are substituted chloride atoms around **2** and **3**, as shown Scheme 1. The absorption and fluorescence spectroscopy of the synthesized SubPc monomer (**1**), dimer (**2**), and trimer (**3**) were measured. We also confirmed the photo-generation of $^1O_2$ by means of UV-vis and obtained the absolute singlet oxygen quantum yields measured in absorption spectra of $^1O_2$. We assumed the cytotoxicity of **1–3** using human HEp2 cells.

EXPERIMENTAL

Measurements

All reactions were induced under N_2 atmosphere. Elemental analyses for carbon, hydrogen, and nitrogen were conducted using a Yanako CHN CORDER MT-6. UV-vis absorption spectra were recorded on a Shimadzu UV-3100 spectrometer. Recyclable preparative high-performance liquid chromatography (HPLC) was carried out on a Japan Analytical Industry Model LC9110 (JAIGEL-2H and 2.5H columns) using $CHCl_3$ as an eluent. Photoluminescence (PL) spectra were recorded on a Shimadzu RF-5300PC spectrofluorometer. ^{1}H NMR spectra were recorded on a JEOL delta ECX-500 spectrometer operating at 500.1 MHz. Chemical shifts for ^{1}H NMR spectra were referenced to $CDCl_3$ (δ = 7.26 ppm). Mass spectra were recorded on a Bruker microTOF using positive mode ESI-TOF method for acetonitrile solutions by using sodium formate as reference. MALDI-TOF-MS spectra were recorded on a Bruker microflex using Dithranol as matrix. Fluorescence quantum yields were evaluated using an absolute PL quantum yield measurement apparatus (C9920-02, Hamamatsu Photonics). A Xenon lamp (Asahi Spectra, MAX-301) was used as a

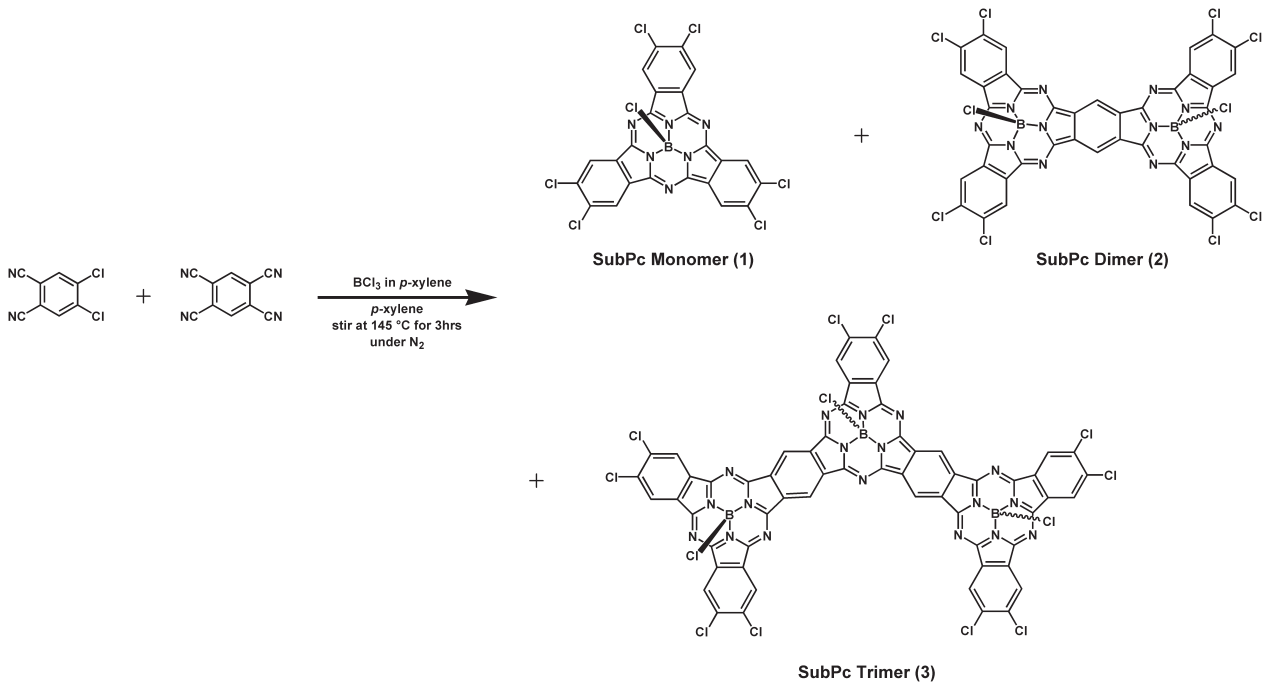

Scheme 1. Synthesis route of subphthalocyanine **1–3**

light source to induce photosensitized singlet oxygen evolution reaction. Light intensities were measured with an optical power meter (ADCMT, 8230E) equipped with an optical sensor (ADCMT, 82311B).

Synthesis

Standard Procedure for the Synthesis od SubPce 1–3

4,5-Dichlorophthalonitrile (1.0 g, 5.3 mmol) and 1,2,-4,5,-tetracyanobenzene (0.4 g, 2.0 mmol) were dissolved in 2 mL of *p*-xylene under N_2. The 2 mL of *p*-xylene solution of Boron trichloride (12.5~14.5 w/w%) were added, and reaction mixture was heated for 3 h at 145 °C. The resulting dark purple slurry was evaporated under vaccuo. The insoluble crude products were removed by silica gel column chromatography with $CHCl_3$/hexane as an eluent. Further purification was achieved by recycling preparative HPLC using $CHCl_3$ as an eluent.

SubPc Monomer (1)

Red purple powder. Yield, 0.33 g (2.8%). *Anal*. Calc. for $C_{24}H_6BCl_7N_6$: C; 45.23, H; 0.95, N; 13.19. Found: C; 45.26, H; 0.73, N; 13.01%. ESI-TOF : Found 678.9143 m/z. (calcd. for $[M+2H+CH_3CN]^+ = 678.9143$). UV-vis (toluene): λ_{max} (ε $mol^{-1}dm^3cm^{-1}$) = 314 (3.7×0^4), 530 (2.8×10^4), 555 (4.9×10^4, sh) and 574 nm (1.0×10^5). ^{1}H NMR ($CDCl_3$): δ = 8.93 ppm (s, α-H).

SubPc Dimer (2)

Dark blue powder. Yield, 6.5 mg (0.30%). *Anal*. Calc. for $C_{42}H_{10}B_2Cl_{10}N_{12}$: C; 47.65, H; 0.95, N; 15.88. Found: C; 47.48, H; 1.02, N; 15.59%. MALDI-TOF: Found 1057.4 m/z. $[M]^+$ (calcd. for $C_{42}H_{10}B_2Cl_{10}N_{12}$ 1057.8). UV-vis (toluene): λ_{max} (ε $mol^{-1}dm^3cm^{-1}$) = 327 (6.4×10^4), 446 (1.6×10^4), 598 (5.2×10^4, sh), 613 (7.1×10^4), 648 (5.5×10^4), 677 (5.8×10^4) and 709 nm (2.2×10^5). ^{1}H NMR ($CDCl_3$): δ = 10.35 (s, 2H, benzo-H), 8.99 (s, 4H, α-H) and 8.91 ppm (s, 4H, α-H).

SubPc Trimer (3)

Blue powder. Yield, 3.2 mg (0.053%). *Anal*. Calc. for $C_{60}H_{14}B_3Cl_{13}N_{18}$: C; 48.69, H; 0.95, N; 17.03. Found: C; 48.42, H; 1.101, N; 16.82%. MALDI-TOF : Found 1479.4 m/z. $[M]^+$ (calcd. for $C_{60}H_{14}B_3Cl_{13}N_{18}$ 1479.8). UV-vis (toluene): λ_{max} (ε $mol^{-1}dm^3cm^{-1}$) = 329 (8.6×10^4), 602 (5.5×10^4), 647 (5.3×10^4), 673 (7.8×10^4), 710 (6.4×10^4), 736 (4.6×10^4), and 777 nm (1.7×10^5). ^{1}H NMR ($CDCl_3$): δ = 10.35 (s, 2H, benzo-H), 10.26 (s, 2H, benzo-H), and 8.93 ppm (m, 10H, α-H).

The singlet oxygen generation

The absolute singlet oxygen quantum yields ($\Phi_{\Delta absolute}$)

The singlet oxygen generation of **1–3** *via* photoirradiation was demonstrated in toluene or dimethyl sulfoxide (DMSO) described in the literature [17]. Sample slutions in quartz cuvette were irradiated with monochromatric light (570, 700 and, 770 nm) through a band-pass filter (Asahi Spectra, MX0570, MX0700, and MX0770) from Xe lump (Asahi Spectra, MAX-300). Sample preparation was carried out in the dark. 1,3-Diphenylisobenzofuran (DPBF) was used as scavenger of active oxygen species in toluene or DMSO. Sample solutions contains 1.5 mL of subphthalocyanine solution at 2.0×10^{-6} M and 1.5 mL of DPBF solution at 2.0×10^{-5} M. The photochemical reactions were followed spectrophotometrically by observing the decrease of absorption peak at 417 nm of DPBF. Quantum yield of decomposition of scavenger ($\Phi_{\Delta absolute}$) was defined as

$$\Phi_{\Delta absolute} = \frac{(number\ of\ decomposed\ scavenger\ molecules)}{(number\ of\ absored\ photon)} \quad (1)$$

and then number of adsorbed photon was calculated from following equation

$$(number\ of\ adsorbed\ photon) = \frac{\Delta E \lambda}{hc} \quad (2)$$

where ΔE was adsorbed energy calculated from power of irradiated light and transmitted light measured with an Optical power meter (ADCMT, 8230E) equipped with an optical sensor (ADCMT, 82311B). λ is wavelength of irradiated light, *h* is Planck constant and *c* are speed of light, respectively.

The relative singlet oxygen quantum yields ($\Phi_{\Delta relative}$)

The relative singlet oxygen quantum yield ($\Phi_{\Delta relative}$) is a relative value determined using the standard value of singlet oxygen quantum yield by the ZnPc in DMSO ($\Phi_{\Delta std.}$ = 0.67) [18–21]. This standard value is generally used in many papers discussing the $\Phi_{\Delta relative}$ of Pcs and their derivatives [22–25]. The $\Phi_{\Delta relative}$ of ZnPc is used as a reference for comparison with other results. The following shows the calculation method of the $\Phi_{\Delta relative}$. The $\Phi_{\Delta relative}$ was defined as

$$\Phi_{\Delta relative} = \Phi_{\Delta std.} \frac{R I_{abs.}^{std.}}{R^{std.} I_{abs.}} \quad (3)$$

where $\Phi_{\Delta std.}$ is the singlet oxygen quantum yield for ZnPc in DMSO ($\Phi_{\Delta std.}$ = 0.67), *R* and $R^{std.}$ are the decompose rates of DPBF in the presence of the SubPc samples and ZnPc, respectively. $I_{abs.}$ and $I_{abs.}^{std.}$ are the rates of light absorption by the SubPc samples and ZnPc, respectively.

Cell study

All cell culture medium and reagents were purchased from Invitrogen (Carlsbad, CA). HEp2 cells were purchased from ATCC and cultured using 50:50 DMEM/Advanced MEM augmented with 10% fetal bovine serum (FBS) and 1% antibiotic (penicillin-streptomycin). A 32 mM stock solution of each SubPc complex was prepared by dissolving in DMSO containing 1% Cremophor EL [26, 27].

Dark Cytotoxicity: HEp2 cells were plated in a Corning Costar 96-well plate and allowed to grow for 48 h at 37 °C under 5% CO_2. The 32 mM **1–3** stock solutions were diluted with culture medium to concentrations of 0, 3.125, 6.25, 12.5, 25, 50, 100 and 200 μM. The cells were treated with **1–3** at the different concentrations (100 μL/well), for 24 h at 37 °C under 5% CO_2. Immediately following incubation the loading medium was removed, and the cells were washed with phosphate-buffered saline (PBS) to remove any residual Pc. The cells were then fed medium containing 20% CellTiter Blue (CTB) (Promega, Madison WI) and incubated for 4 h. Cell viability was determined by fluorescence intensity at 570/615 nm using a BMG FLUOstar OPTIMA microplate reader. Cell dark cytotoxicity is expressed as a percentage of viable cells.

***Photocytotoxity*:** HEp2 cells were plated and allowed to grow as described above. The SubPc concentrations used for testing phototoxicity were 0, 3.125, 6.25, 12.5, 25, 50 and 100 μM. As for the dark toxicity assay, the cells were treated with **1–3** and incubated at 37 °C under 5% CO_2 for 24 h. Immediately following incubation the loading medium was removed and the cells were washed with PBS to remove any residual SubPcs. The cells were then fed fresh medium and exposed to light for 20 min using a 600W Quartz Tungsten Halogen lamp (Newport Corporation, Irvine CA) to generate a light dose of approximately 1.5 J/cm^2. During light exposure, the plate was chilled using an Echotherm IC50 chilling/heating plate (Torrey Pines Scientific, Carlsbad CA) set to 5 °C to maintain ambient temperature. Following light exposure the cells were incubated for another 24 h, after which the media was removed and replaced with medium containing 20% CTB and subsequently incubated for 4 h. The cell viability was determined by fluorescence intensity at 570/615 nm using a BMG FLUOstar OPTIMA microplate reader. The cell phototoxicity is expressed as a percentage of viable cells.

RESULTS AND DISCUSSION

Synthesis and characterization

SubPc monomer **(1)**, dimer **(2)** and trimer **(3)** were prepared from commercially available 4,5-dichlorophthalonitrile, 1,2,4,5,-tetracyanobenzene, and BCl_3 compounds into a *p*-xylene solution using the method

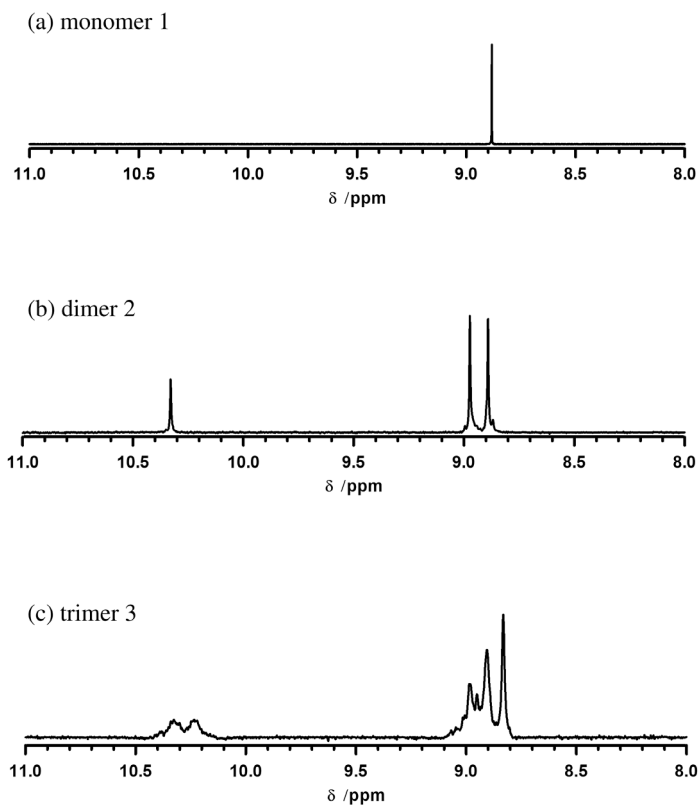

Fig. 1. ^{1}H NMR spectra of SubPcs **1–3** in $CDCl_3$

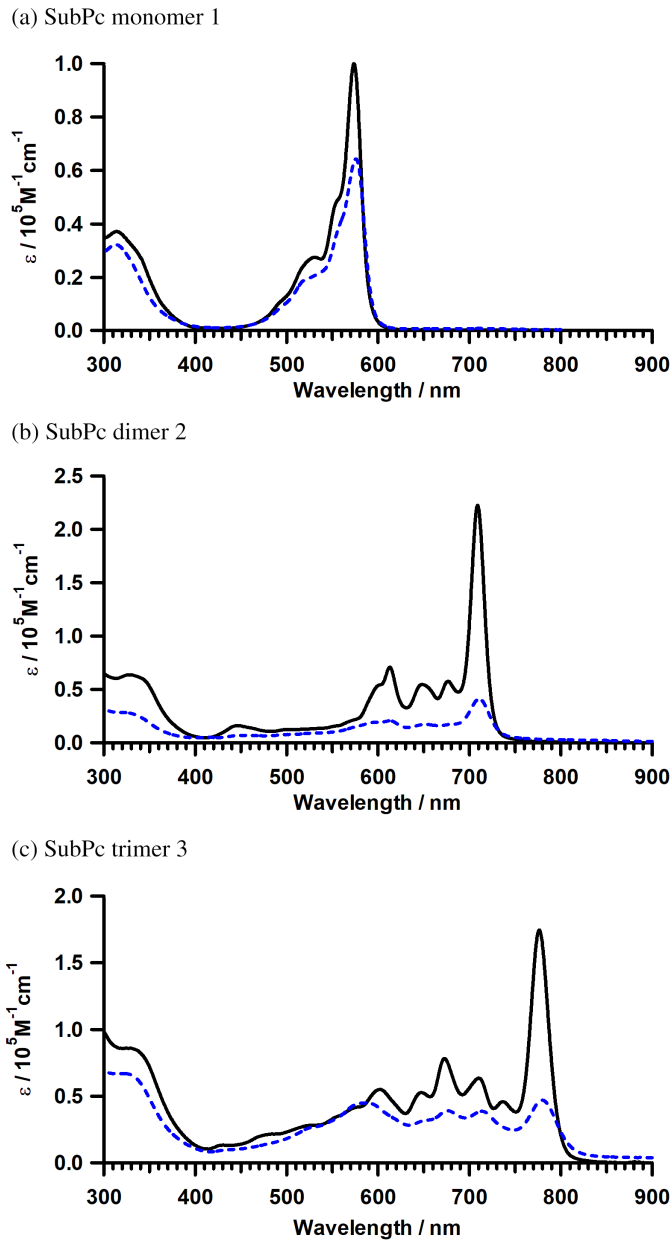

Fig. 2. Absorption spectra of SubPcs **1–3** in toluene and DMSO. (**black line** : in toluene, **blue line** : in DMSO)

previously described in the literatures [15, 16, 28]. The macrocyclization reaction of **1–3** was performed in *p*-xylene, and produced crude products were subsequently purified by silica gel column chromatography. Final isolation and purification were achieved by the recycling preparative HPLC using $CHCl_3$ as an eluent. The isolated yields of **1**, **2** and **3** were 2.8, 0.30 and 0.053%, respectively. SubPcs **1–3** show high solubility in organic solvents such as CH_2Cl_2, $CHCl_3$, and toluene. They also dissolve in polar solvents such as methanol and DMSO.

Elemental analysis and spectroscopic data (^{1}H NMR and MALDI-TOF mass spectra) confirmed the assigned structures for **1–3**. The results of these analyses were consistent with the assigned structures, as shown in the Scheme 1. The ^{1}H NMR spectra of **1–3** are shown in Fig. 1. The ^{1}H NMR spectrum of **1** was measured in $CDCl_3$ at R.T. and showed only the sharp singlet signal of the α-proton of the SubPc ring at δ = 8.93 ppm. In the ^{1}H NMR spectrum of **2** in $CDCl_3$, the α-proton signals of the SubPc ring units appeared as two signals at δ = 8.99 and 8.91 ppm with an integral value of 4 protons, respectively. In addition, a sharp singlet signal for the benzo ring which links two SubPc ring units are observed at δ = 10.35 ppm with an integral value of 2 protons. The ^{1}H NMR spectra of **3** was also measured in $CDCl_3$ and showed multiplet signal at δ = 8.93 ppm with an integral value of 10 protons of the SubPc ring units. Also, two singlet signals at δ = 10.35 and 10.26 ppm, respectively with an integral value of 2 protons of benzo ring which links two SubPc ring units. Upon purification of **2** and **3**, the measurment of the ^{1}H NMR spectra showed that **2** had one of the two isomers (syn or anti) and **3** had several isomers [15, 16].

Absorption and Fluorescence spectra

The UV-vis spectra of **1–3** in toluene are shown in Fig. 2. The results of the UV-vis and fluorescence spectra of **1–3** in toluene are listed in Table 1. In 1.5×10^{-5} M, the Q-bands of **1** were observed as a sharp absorption band 574 nm and fluorescence emission of **1** appeared at 584 nm. In Dimer **2**. The Q-bands and fluorescence emission of **2** were observed at 709 nm and 712 nm, respectively. In Trimer **3**, The Q-bands of **3** were observed at 777 nm with significant red shifts in comparison with **1** and **2** and fluorescence emission of **3** were appeared at 784 nm. The red shifts of absorption and fluorescence spectra in SubPcs **1–3** are owing to the expansion of π conjugated system in core units. The absolute fluorescence quantum yield (Φ_F) of SubPcs **1–3** also measured, Φ_F values were 39.0 for **1**, 25.9 for **2** and 18.9% for **3**, respectively. These spectroscopic properties of **1–3** were consistent with the characteristics of previously reported SubPc analogs [15, 16, 28].

UV-vis spectra of **1–3** measured at 1.5×10^{-5} M in DMSO are shown in Fig. 2. These results were compared to those of the absorption spectra measured in toluene, which exhibited large decreses of absorbance

Table 1. Photophysical and photochemical parameters of SubPcs **1–3** in toluene at 1.5×10^{-5} M

Comp.	λ_{max} (nm)	λ_{Em} (nm)	SS (nm)	Φ_F (%)
Monomer 1	574	584	10	39.0
Dimer 2	709	712	3	25.9
Trimer 3	777	784	7	18.9

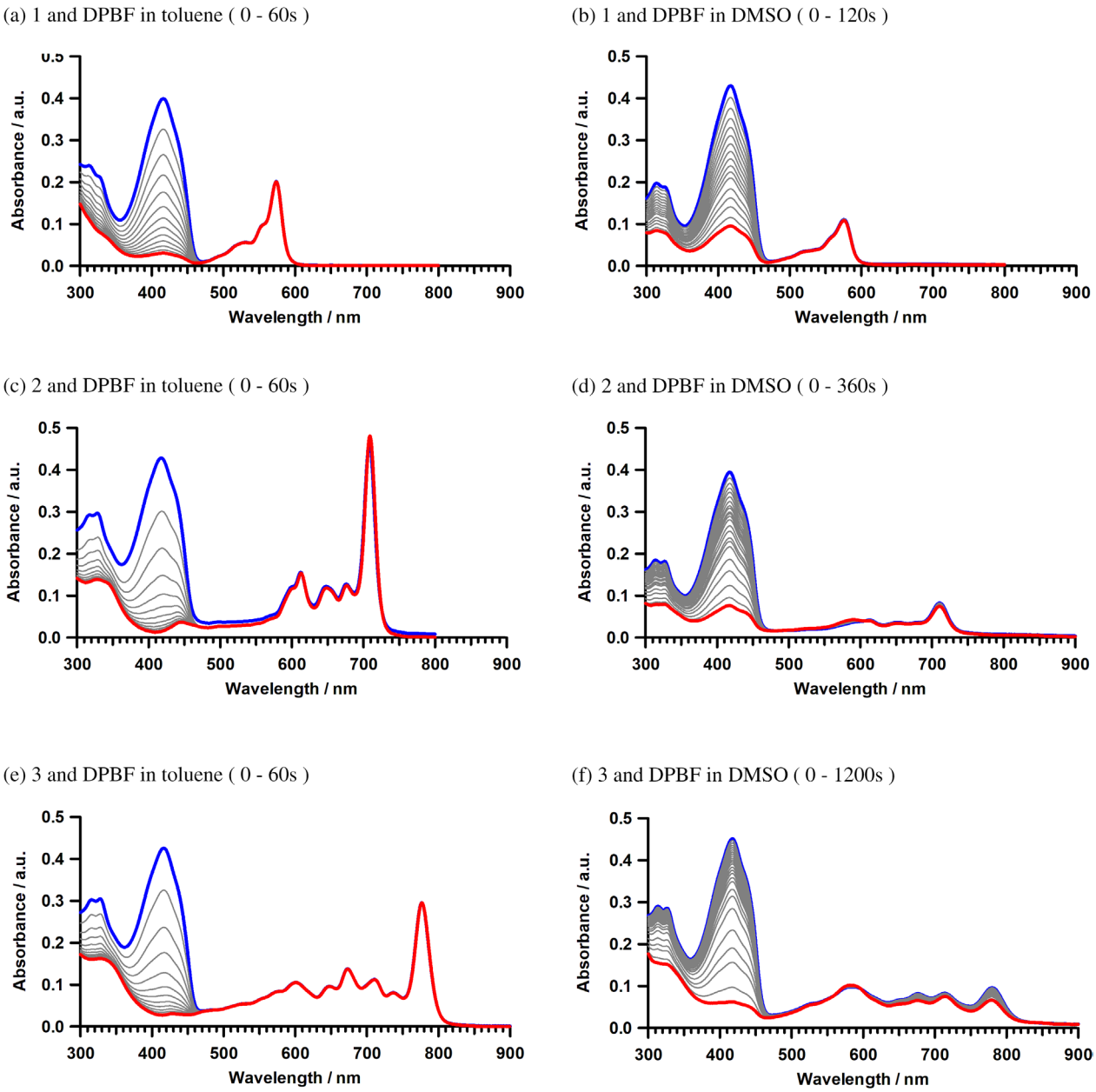

Fig. 3. The absorption spectral changes of SubPcs **1–3** during photo irradiations in toluene and DMSO. (Wavelength of irradiation lights; SubPc **1** (a and b): 570 nm, SubPc **2** (b and c): 700 nm, SubPc **3** (d and e: 770 nm)

levels in the spectra. In the case of highly planar Pcs, such a decrease in absorbance level is due to the formation of aggregates in the solvent. In addition, when using an aggregate of Pcs, new absorption bands are observed. However with SubPcs, no absorption bands derived from the aggregate are observed [15, 16]. Actually, due to the steric structure of the subphthalocyanine rings, it is very difficult for the subphthalocyanine rings to form aggregates in the solution.

In order to clarify the differences between the absorption spectra in DMSO, the absorption bands were measured at concentrations from 2.0×10^{-6} M to 2.0×10^{-5} M, respectively. The results of changes in absorption bands due to concentration are shown in S2. SubPcs **1–3** were found to obey Lambert-Beer's law in DMSO up to 2.0×10^{-5} M. From these results, we conclude that the difference between the absorption spectra in toluene and the absorption spectra in DMSO were due to the difference in their solvent polarities.

Singlet oxygen generation properties

Scheme 2 shows the PDT photo reaction mechanisms. The Type I reaction leads to the formation of free radicals such as the superoxide anion radical ($O_2^{-\bullet}$) and the hydroxyl radical ($OH^{\bullet}$). On the other hands, the Type II

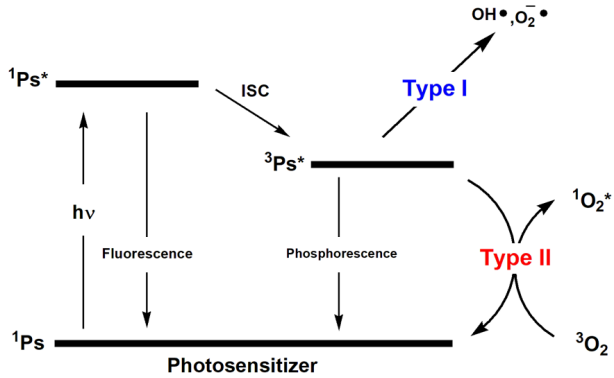

Scheme 2. The reaction mechanism of PDT

Table 2. The values of the absolute singlet oxygen quantum yields ($\Phi_{\Delta absolute}$) of SubPcs **1–3**

SubPc	Solvent	$\Phi_{\Delta absolute}$ [%]	$\Phi_{\Delta relative}$ [%]
Monomer 1	Toluene	20.4	—
	DMSO	8.65	56
Dimer 2	Toluene	15.8	—
	DMSO	7.75	50
Trimer 3	Toluene	14.6	—
	DMSO	2.38	15
ZnPc	DMSO	10.3	67[a]

[a]Data from Ref. [21].

reaction leads to the formation of singlet oxygen. Finally, The generated reactive oxygen species (ROS) *via* photo reaction attacks the tumor cells [9–11].

The singlet oxygen ($^1O_2$) generation abilities of **1–3** upon light irradiation *via* a Type II mechanism were measured to evaluate those efficiencies of **1–3** as PDT photosensitizers. The evaluations of $^1O_2$ generation abilities of **1–3** were applied absolute singlet oxygen quantum yields ($\Phi_{\Delta absolute}$). The values of $\Phi_{\Delta absolute}$ were determined by a chemical method using 1,3-diphenylisobenzofuran (DPBF) as $^1O_2$ scavenger. The $\Phi_{\Delta absolute}$ obtained from the oxidative decomposition of DPBF by the $^1O_2$ generated through photoirradiation of **1–3**. The $\Phi_{\Delta absolute}$ was calculated using Eq. (1) taking into account the number of molecules of decomposed DPBF and the photon number absorbed by **1–3**. The number of molecules of decomposed DPBF was calculated from the slope of absorbance derived from DPBF. The slope was applied the value in range where keeps a linear. The photo reactions of **1–3** were performed in toluene and DMSO. They were performed by irradiating with 570, 700, and 770 nm light corresponding to each Q-band. The observed changes of the UV-vis spectra during irradiation for sample solutions are shown in Fig. 3. The values of the $\Phi_{\Delta absolute}$ of SubPcs **1–3** are listed in Table 2. The details of the slope of absorbance derived from DPBF are shown in supporting information (S1).

In the reaction between **1** and DPBF in toluene, the absorption band at around 417 nm derived from DPBF was observed greate decrease of intensity of absorbance during photo irradiation. In the photo reactions with same reaction manner of **2** and **3** having red-shifted Q-band absorption up to near-IR region, greate decrease of absorption band around at around 417 nm also were observed. These results indicated that the light irradiation of **1–3** induces the generation of $^1O_2$ and decomposition of DPBF. $\Phi_{\Delta absolute}$ for DPBF in toluene were calculated to be 20.4 for **1**, 15.8 for **2** and 14.6% for **3**, respectively. As a result of calculations of $\Phi_{\Delta absolute}$ of SubPcs **1–3** for DPBF in toluene, it is founded that $\Phi_{\Delta absolute}$ decrease with increments of size of molecules. The energy loss due to the non-irradiation process such as molecular vibration could be suggested a factor for the decrease of $\Phi_{\Delta absolute}$ [17].

The photo reactions between **1–3** and DPBF also occered in DMSO. In DMSO of **1–3**, the absorption intensities of **1–3** were lower than those of the toluene solution. Only **1** or **2** combined with DPBF in DMSO showed a decrease of the absorption band at around 417 nm derived from DPBF during photo irradiation. On the other hand, **3** combined with DPBF in DMSO showed a decrease of the absorption band derived from DPBF and of the Q like-band of **3**. This result indicates that the trimer is unstable to irradiation in DMSO. The $\Phi_{\Delta absolute}$ for values for SubPcs **1–3** were calculated to be 8.65 for **1**, 7.75 for **2** and 2.38% for **3**, respectively. The $\Phi_{\Delta absolute}$ values for non-substituted zinc phthalocyanine (**ZnPc**) have been reported 10.3% in similar reaction conditions [17]. Comparison of the $\Phi_{\Delta absolute}$ values showed the $\Phi_{\Delta absolute}$ values of **1–3** to be lower than $\Phi_{\Delta absolute}$ value of ZnPc. The smaller $\Phi_{\Delta absolute}$ values obtained for SubPcs **1–3** could be caused by the decrease in the intensity of the absorption band due to the more polar solvent DMSO.

We also calculated the relative singlet oxygen quantum yields ($\Phi_{\Delta relative}$) of **1–3** using a standard value for the oxidative decomposition of DPBF by **ZnPc** through photo irradiation. The calculation method of $\Phi_{\Delta relative}$ was used the method previously described in the literature using the standard value ($\Phi_{\Delta std.} = 0.67$) [18–21]. This standard value is generally used in many papers discussing $\Phi_{\Delta relative}$ of phthalocyanine. This method is generally used obtaining the $\Phi_{\Delta relative}$ of Pcs [23, 24]. The $\Phi_{\Delta relative}$ of **1–3** were 56 for **1**, 50 for **2** and 15% for **3**, respectively. Regardless of formation of aggregations, the $\Phi_{\Delta relative}$ values of monomer **1** and dimer **2** are similar to those reported for non-aggregated metal Pc complexes [29–31].

3.4 *Cytotoxicity*

The dark toxicity and photocytotoxicity of **1–3** were evaluated in human carcinoma HEp2 cells using the Cell

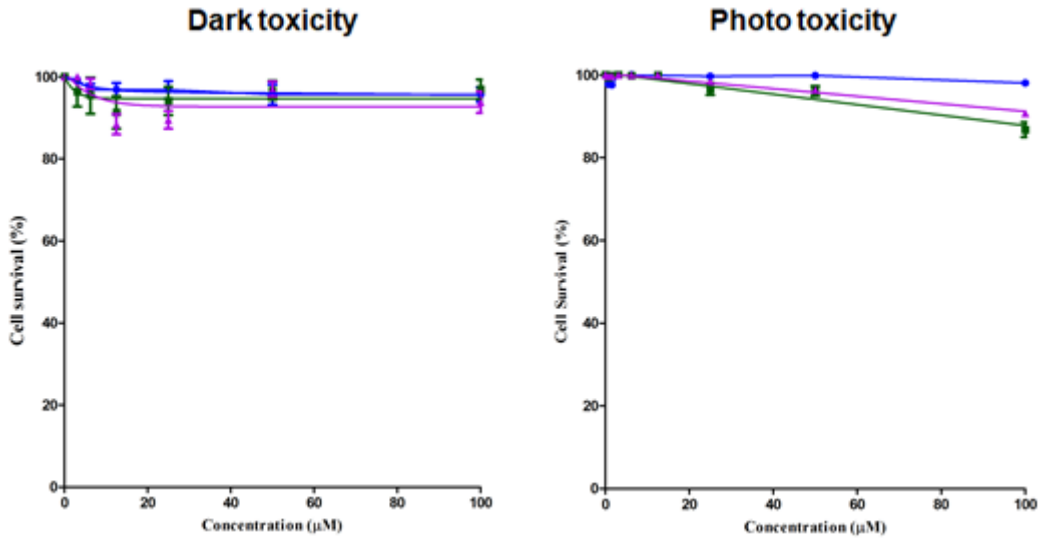

Fig. 4. The cytotoxicity of SubPcs **1**–**3** for HEp2 cell. ●: SubPc **1**, ▪: SubPc **2**, ▲: SubPc **3**

Titer Blue assay [17, 26, 27]. Various concentrations of **1–3** up to 100 μM were evaluated in this study. The results of these studies are summarized in Fig. 4. The dark toxicity results for **1**–**3** showed that all compounds are nontoxic toward HEp2 cells in the dark. The phototoxicity of **1–3** were investigated using photo-irradiation with a low light dose of approximately 1.5 J/cm^2 and also showed the almost negligible toxic properties of **1–3** toward HEp2 cells. We assumed that **1–3** lack sufficient solubility to penetrate HEp2 cells.

Acknowledments

The authers are grateful to Dr. Michiko Egawa (Shimane University) for her measurements of elemental anarysis. Thanks are due to the Reserch Center for Molecular-Scale Nanoscience, the Institute for Molecular Science (IMS), Okazaki Japan. We also thank kind supports from Prof. Hiromitsu Maeda (Ritsumeikan University) for MALDI-TOF-MS measurements.

REFERENCES

1. Meller M and Ossko A. *Monatsh. Chem.* 1972; **103**: 150–155.
2. Claessens CG, González-Rodríguez D and Torres T. *Chem. Rev.* 2002; **102**: 835–853.
3. Claessens CG, González-Rodríguez D, Rodríguez-Morgade MS, Medina A and Torres T. *Chem. Rev.* 2014; **114**: 2192–2277.
4. Kobayashi N. *Synthesis and Spectroscopic Properties of Phthalocyanine Analogs, The Porphyrin Handbook*, Vol. 15. Academic Press: San Diego, 2003; 161–262.
5. Yano S, Hirohara S, Obata M, Hagiya Y, Ogura S, Ikeda A, Kataoka H, Tanaka M and Joh T. *J. Photochem. Photobiol. C: Photochemistry Reviews,* 2012; **12**: 46–67.
6. Zhao J, Wu W, Sun J and Guo S. C*hem. Soc. Rev.,* 2013; **42**: 5323–5351.
7. Hu W, Xie M, Zhao H, Tang Y, Yao S, He T, Ye C, Wang Q, Lu X, Huangbd W and Fan Q. C*hem. Sci.,* 2018; **9**: 999–1005.
8. Bonnett R. *Chemical Aspects of Photodynamic Therapy*, Gordon and Breach Science Publishers: Amsterdam, 2000.
9. Sternberg ED, Dolphin D and Brückner C. *Tetrahedron,* 1998; **54**: 4151–4202.
10. Dougherty TJ, Gomer CJ, Henderson BW, Jori G, Kessel D, Korbelik M, Moan J and Peng Q. *J. Natl. Cancer Inst.,* 1998; **90**: 889–905.
11. Gerdes R, Wöhrle R, Spiller W, Schneider G, Schnurpfeil G and Schulz-Ekloff G. *J. Photochem. Photobiol. A*: *Chemistry,* 1997; **111**: 65–74.
12. McKeown NB. *Phthalocyanine Materials: Synthesis, Structure and Function,* Cambridge University Press: Cambridge, 1998.
13. Dumoulina F, Durmus M, Ahsena V and Nyokong T. *Coord. Chem. Rev.,* 2010; **254**: 2792–2847.
14. Baygu Y and Gök Y. *Inorg. Chem. Commun.,* 2018; **96**: 133–138.
15. Claessens CG and Torres T. *Angew. Chem. Int. Ed.,* 2002; **41**: 2561–2565.
16. Fukuda T, Stork JR, Potucek RJ, Olmstead MM, Noll BC, Kobayashi N and Durfee WS. *Angew. Chem. Int. Ed.,* 2002; **41**: 2565–2568.
17. Fujishiro R, Sonoyama Y, Ide Y, Fujimura T, Sasai R, Nakgai A, Mori S, Kaufman EM, Vicente MGH and Ikeue T, *J. Inorg. Biochem.*, 2019; **192**: 7–16.

18. Fery-Forgues S and Lavabre D. *J. Chem. Ed*., 1999; **76**: 1260.
19. Seotsanyana-Mokhosi I, Kuznetsova N and Nyokong T. *J. Photochem. Photobiol. A. Chem*. 2001; **140**: 215–222.
20. Yank D, Aydin M, Durmus M and Ahsen V. *J. Photochem. Photobiol. A*. 2009; **206**: 18–26.
21. Kuznetsova N, Gretsova N, Kalmykova E, Makarova E, Dashkevich S, Negrimovskii VV, Kaliya O and Luk'yanets E. *Russ. J. Gen. Chem.* 2000; **70**: 133–140.
22. Nyokong T. *Cood. Chem. Rev*., 2007; **491**: 1–9.
23. Sen P, Managa M and Nyokong T. *Inorg, Chem, Acta.*, 2019; **251**: 1707–1722.
24. Nene LC, Managa M and Nyokong T. *Dyes Pigm*., 2019; **165**: 488–498.
25. Ogunsipe A, Chenb J and Nyokong T. *New. J. Chem.*, 2004; **28**: 822–827.
26. Li H, Jensen TJ, Fronczek FR and Vicente MGH. *J. Med. Chem.,* 2008; **51**: 502–511.
27. Iglesias RS, Claessens CG, Torres T, Herranz MÁ, Ferro VR and García de la Vega JM. *J. Org. Chem.,* 2007; **72**: 2967–2977.
28. Shibata N, Mori S, Hayashi M, Umeda M, Tokunaga E, Shiro M, Sato H, Hoshi T and Kobayashi N. *Chem. Commun.,* 2014; **50**: 3040–3043.
29. Camur M, Ahsen V and Durmus M. *J. Photochem. Photobiol.,* 2011; **219**: 217–227.
30. Durmus M and Ahsen V. *J. Inorg. Biochem.*, 2010; **104**: 297–309.
31. Oliweole DO, Sari FA, Prinslon E, Dube E, Yuzer A, Nyokong T and Ine M. *Spectrochim. Acta A Mol. Bionol. Spectrosc.,* 2018; **203**: 236–243.